Consistency Driven Respiratory Phase Alignment and Motion Compensation in PET/CT

Adam Alessio, *Member, IEEE*, Steve Kohlmyer, Paul Kinahan, *Senior Member, IEEE*

***Abstract*—Respiratory motion in PET/CT imaging degrades PET image quantitation due to misaligned attenuation correction (AC) factors and motion blurring. This work explores the use of the Radon consistency conditions to compensate for these limitations in respiratory gated PET images in which only a single CT scan is available for AC. Specifically, we use the Radon consistency of AC-PET data as a metric to transform the attenuation map to match each phase of respiratory gated data, perform phase matched AC, and then use the inverse of the transformation parameters to align the gated PET images into a single phase. A final image volume is formed from summing PET images aligned to a single phase. We test this method with three transformation types applied to simulated data and measured patient PET/CT data. Results show successful alignment of attenuation maps and minor quantitative improvement with the proposed methods.**

I. Introduction

Respiratory gated whole-body PET imaging is available with many commercial PET/CT systems. These systems use external motion tracking devices to gate the PET data into independent respiratory bins. The measurements in each respiratory bin must be corrected for attenuation. Phase-matched attenuation correction (AC) using respiratory gated PET and CT has been proposed, but this requires identical patient movement during PET and CT imaging and additional radiation exposure for gated CT. To avoid these challenges and for ease of operation, the attenuation correction map is usually formed from a single helical CT acquisition, which is effectively a snap-shot of a single time point in the respiratory cycle. In this imaging scenario, the attenuation map is misaligned with some or all of the bins of respiratory gated PET data. This work attempts to compensate for attenuation correction and motion errors with respiratory gated PET images using a single helical CT scan.

The proposed method contains the following steps:

1) Use the Radon consistency of AC-PET data as a metric to find the optimal transformation of the CT attenuation map to match each gate of respiratory gated PET data,
2) Perform phase-matched AC,
3) Use the inverse of the transformation parameters to align the gated PET images into a single respiratory gate.
4) Sum PET images after they have been aligned to a single gate.

Manuscript for 2007 IEEE NSS/MIC proceedings received October 29, 2007. This work was supported by NIH grants HL086713 and CA115870.

A. Alessio and P. Kinahan are with the Dept. of Radiology, University of Washington, Seattle, WA 98195 USA. (telephone: (206)543-2419, email: aalessio@u.washington.edu)

S. Kohlmyer is with GE Healthcare, Waukesha, WI.

We test this method with three transformation types applied to simulated data and measured patient PET/CT data. This is an extension of our previous work using simple attenuation alignment for cardiac PET/CT [1]. Results show modest quantitative improvement with the proposed methods for single respiratory bins and litte to no improvement in summed images.

II. Attenuation Correction Alignment Metric

The proposed methods align a single attenuation map (formed from scaling a CT image volume to PET energy) to each phase of respiratory gated PET data. The automatic alignment is performed by transforming the attenuation map until the AC-PET data optimally meet the two-dimensional Radon consistency conditions. This work uses a metric originally proposed by Welch et al for conventional PET imaging [6]. Their work used an alignment metric which tests the first three moments of the Helgason-Ludwig consistency conditions on 2-D Radon transforms. We employ Natter's formulation of the consistency conditions

$$\int_0^{2\pi}\int_{-\infty}^{\infty} s^m e^{ik\phi} e^{T(s,\phi)} E(s,\phi) ds d\phi = 0 \qquad (1)$$

where $E(s,\phi)$ are the measured data, $T(s,\phi)$ are the projections of the attenuation image, $m \geq 0$ is the moment, and k is the Fourier component [2]. We find a transformed attenuation image which leads to AC-PET data that minimizes sum of the values from the left side of equation (1) for $m = 0, 1, 2$ and when $k > m$ or $m + k$ is odd.

III. Transformation Methods

This work proposes and tests three transformation schemes for the attenuation map catering to respiratory gated PET data. Method 1 uses a **rigid** body transformation allowing for translations in x, y, z and a rotation around the x axis. Method 2 uses an **affine** transformation allowing for translations in x, y, z and expansion along the y axis (anterior-posterior) and z axis (axial). For these methods, the optimal attenuation map for each phase was found with a simplex search algorithm that preferentially searches the dimensions which are expected to have more variation from respiration (z translation, y, z expansion). At each iteration, the current transformed attenuation map is forward projected and applied as attenuation correction to the measured PET data. The consistency of the AC-PET data is assessed with equation (1), and then another set of transformation parameters is tested. The simplex algorithm iterates over transformation variables until it converges to an

optimal transformation. The optimal transformation parameters offer knowledge of the motion between each respiratory bin. For each phase, we apply the inverse of the attenuation map transformation to the respiratory gated PET image to transform all the gated PET images to a single phase. Then, all of the single phase PET images are summed. This alignment and summation attempts to remove motion blurring.

Method 3 uses a simple non-rigid transformation which selects the optimal slice from the entire attenuation map for each slice of each phase of the respiratory gated data. This **match slice** approach is based on the assumption that the majority of respiratory motion is along the axial direction and that some slices from the CT image may better match a different slice from the PET data. Unlike the previous two methods, we do not invert this non-rigid transformation and apply it to the PET images prior to summing the separate bins because this non-rigid approach does not insure conservation of mass/activity and may lead to unrealistic PET images.

IV. Evaluation Methods

We tested the alignment process with simulations of respiratory gated PET from the NURBS-based Cardiac Torso (NCAT) phantom[5]. We simulated tidal breathing with a 1.5cm max diaphragm range (0.8cm chest expansion) and a 1cm moving right pulmonary lesion with a 10:1 tumor to background activity ratio. The activity concentration in each organ were set to match relative FDG uptake according to average SUV values from literature [3], [4]. We added noise to the simulated data to model the first order influence of photon detection and scatter. A single CT scan for attenuation correction was modeled with a noise-free attenuation map from end tidal inspiration. This single map was transformed with the three proposed methods to match the PET data from each respiratory bin.

We also tested these methods with patient data from a whole body FDG PET/CT study using our current clinical protocol. The PET data was respiratory phase gated into 5 bins and a single helical CT scan was performed during normal tidal breathing.

V. Results from Simulations

Figures 1 and 2 display moments of projection data from a single slice of the NCAT phantom. These moments (integral over s in equation 1) versus azimuthal angle reveal the frequency content of higher order moments and visually support the proposed formulation of the Radon consistency conditions. The Fourier transform in ϕ of these curves (integral over ϕ in equation 1, in practice the discrete Fourier transform) will have coefficients at k, equal to zero when $k > m$ and $k+m$ is odd. Each figure plots the moments of simulated projection data when "Perfect AC" is applied, when "No AC" is applied, when end tidal inspiration attenuation correction applied to end tidal expiration "Current Practice", and when the end inspiration attenuation map is rigid-body registered to PET data with the proposed method "Rigid".

These moment figures visually reveal that attenuation correction is required for consistency ("No AC" does not follow behavior of "Perfect AC"). Also, misaligned attenuation correction resulted in a slight perturbation from consistent data ("Current Practice" is not identical to "Perfect AC"). Furthermore, the rigid body alignment method resulted in moments slightly closer to "Perfect AC" than the "Current Practice" suggesting improved alignment of the attenuation map after the rigid body transformation. Finally, the presence of noise does not change the underlying structure of these moments.

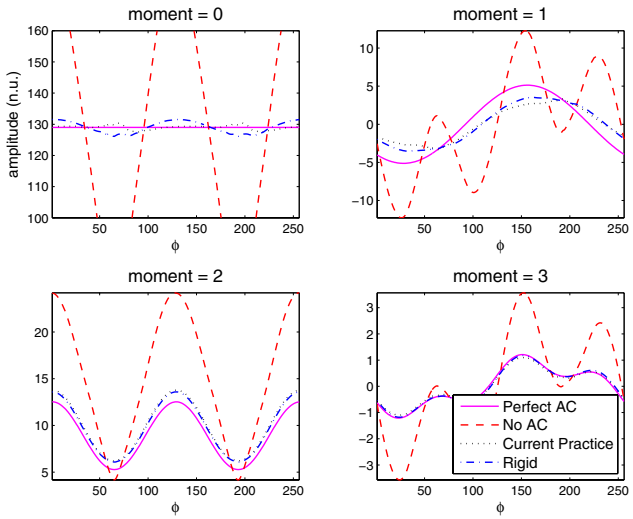

Fig. 1. Moments of noise-free projection data from a single slice of NCAT phantom versus azimuthal angle reveal the periodicity of higher order moments and conceptually support the proposed formulation of the Radon consistency conditions. Curves are presented in normalized units.

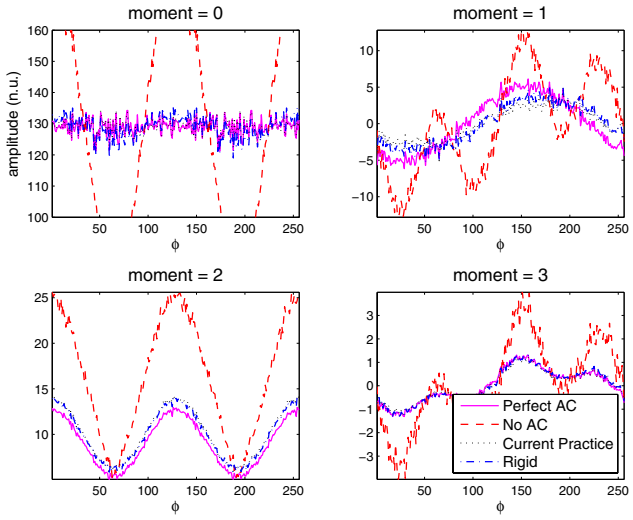

Fig. 2. Moments of noisy projection data from a single slice of NCAT phantom versus azimuthal angle.

Images from noise-free NCAT simulations appear in figure 3. Figure 3b shows a coronal view through a single phase of the respiratory gated PET images using the original attenuation map. This view reveals the common "banana" artifact along the diaphragm due to attenuation mismatch. The proposed methods lead to slightly reduced banana artifacts, but still contain other artifacts including erroneous hot and

cold spots due to attenuation mismatch in the lung space (Figures 3d, e and f). Figure 4 plots the global mean square error (MSE), the MSE of the diaphragm slices, and the bias in the right tumor for each method. Respiratory bins 1 and 8 correspond to expiration phases which are poorly matched with the inspiration phase (5) attenuation map. In general, the proposed methods slightly improve off phase bins.

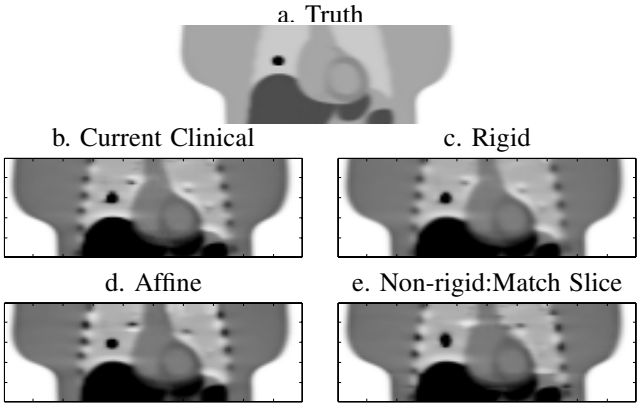

Fig. 3. Coronal view of image volumes reconstructed from simulated noise-free, respiratory gated data. Attenuation correction was performed with a single helical scan (b), with rigid body AC alignment (c), with affine AC alignment (d), and with the match slice method (e). Each of the 8 respiratory bin images were then transformed to a single phase based on attenuation map deformation and summed.

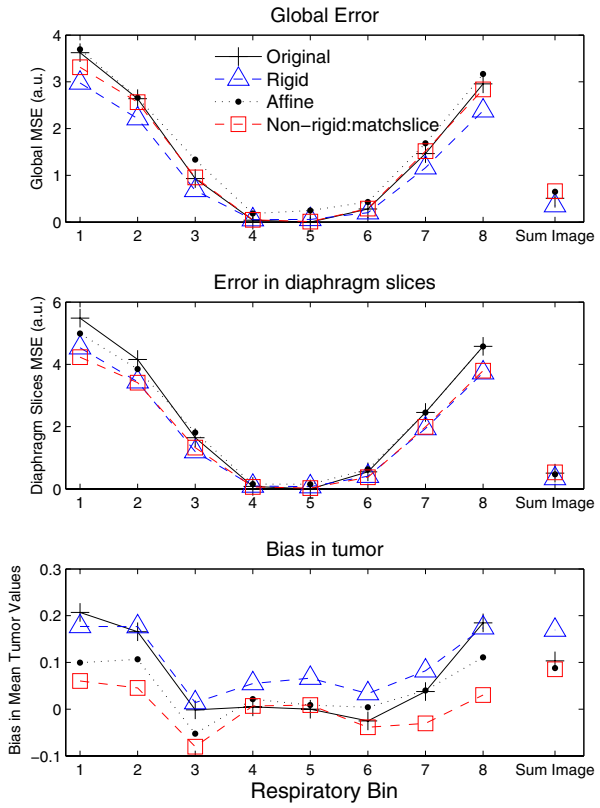

Fig. 4. Plots of error derived from noise-free NCAT simulations. Values are plotted for each respiratory bin and for the image transformed and summed over all phases.

Images from a single phase of noise present NCAT simulations appear in figure 5. After phase-matched attenuation correction and reconstruction, each of the 8 respiratory bin images were either transformed to a single phase based on attenuation map deformation (Rigid and Affine methods) and summed, or just summed (Current Clinical practice and Match Slice method). Final summed images appear in figure 6. Quality metrics for each respiratory bin and the final summed image appear in figure 7. There is some reduction in error with the Rigid and Match Slice method for individual respiratory bins, but bias in the tumor is actually worse with these methods. The proposed methods to not offer appreciable gains in the final summed image.

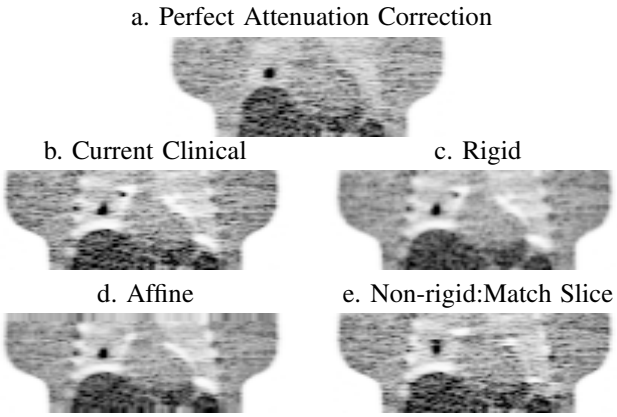

Fig. 5. Coronal view of image volumes reconstructed from simulated end tidal expiration, respiratory gated data in the presence of noise (bin 1 of 8). Attenuation correction was performed with a single helical scan from end inspiration (b), with rigid body AC alignment (c), with affine AC alignment (d), and with the match slice method (e).

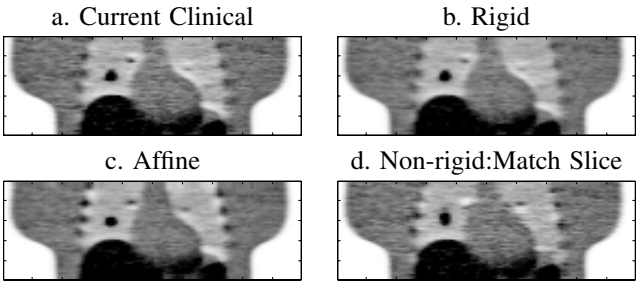

Fig. 6. Coronal view of image volumes reconstructed from simulated respiratory gated data and summed across respiratory bins. Attenuation correction was performed with a single helical scan (a), with rigid body AC alignment (b), with affine AC alignment (c), and with the match slice method (d). Each of the 8 respiratory bin images were then transformed to a single phase based on attenuation map deformation and summed.

VI. Results from Patient Studies

Figure 8 plots the objective function for the rigid alignment of one respiratory bin and shows that, even with noisy PET data, this function has a global minima. Figure 9 presents images from a single respiratory bin. The alignment methods lead to new attenuation maps at each respiratory phase. Cine movies of these attenuation maps reveal expected respiratory motion and offer a level of confidence in the success of the alignment process. Figure 10 plots the maximum value of the most superior, right diaphragm tumor for each respiratory bin

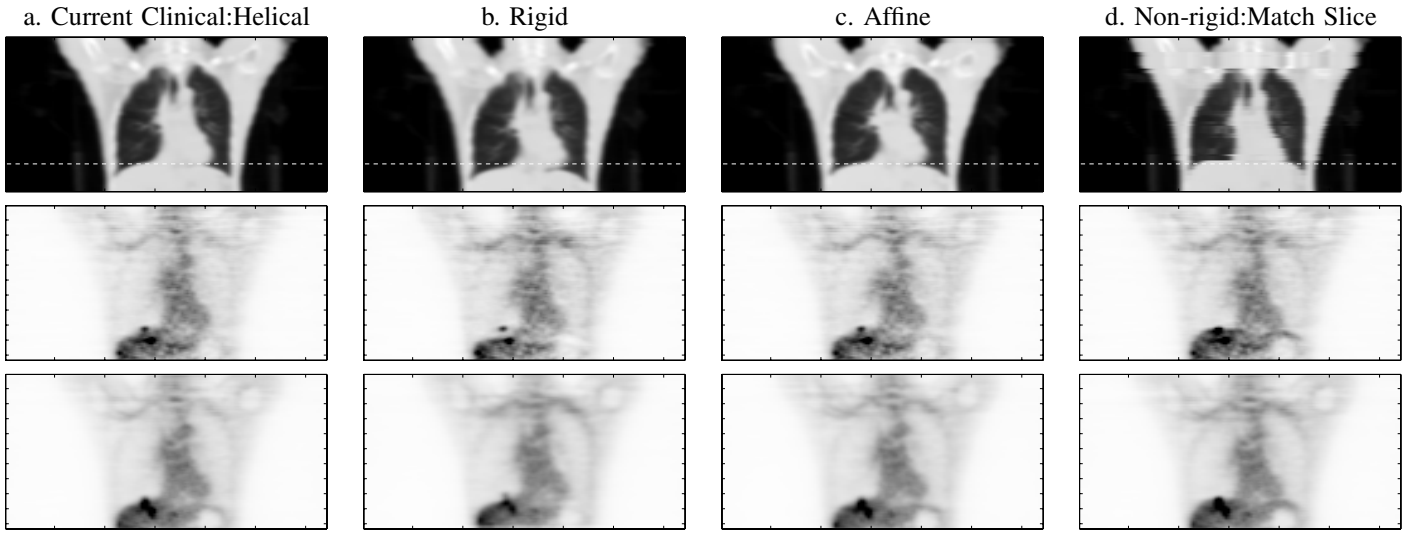

Fig. 9. Coronal views of attenuation map transformed to respiratory bin 1 of 5 (row 1), AC-PET image from bin 3 of 5 (row 2), and PET image summed across all 5 respiratory bins (row 3). The PET images were attenuation corrected either with a single helical CT, similar to current clinical practice (a), or with different transformations of the single attenuation map to each phase (b,c,d).

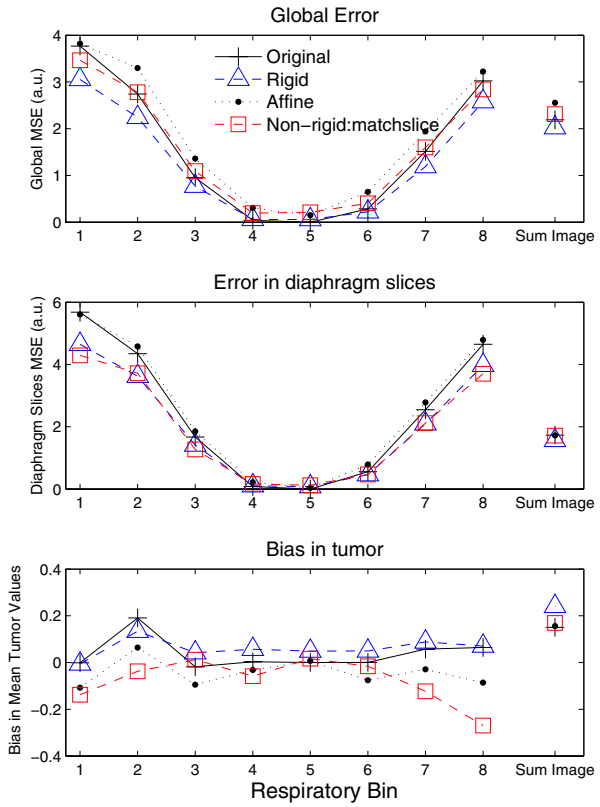

Fig. 7. Plots of error derived from noise present NCAT simulations. Values are plotted for each respiratory bin and for the image transformed and summed over all phases.

and for the summed image. This tumor was selected because attenuation mismatch along the diaphragm is known to cause quantitative inaccuracies and cine movies of respiratory motion in this patient reveal 1-2cm of axial motion for this tumor. The non-rigid approach lead to the highest maximum values and to the most normalized tumor values across respiratory bins. With this metric, the other methods offered equal or worse performance than a conventional helical CT.

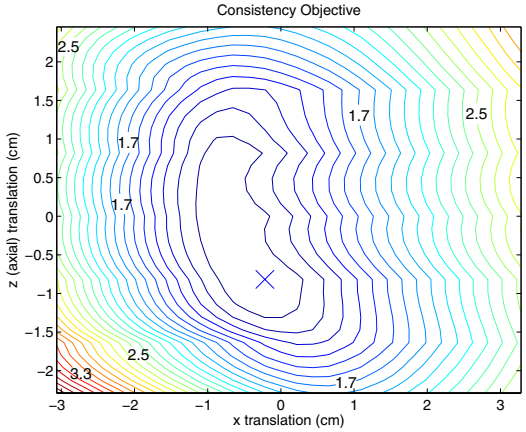

Fig. 8. Values of objective function for different of z and x translations of the attenuation map which is then applied as AC factors for a single respiratory phase from the patient study. Plot reveals that even with noisy respiratory gated data, the consistency metric offers enough information for a global minima (designated with 'X').

VII. Conclusion

We developed alignment methods for providing phase-matched attenuation correction for respiratory gated PET data using a single CT scan. In simulated and measured PET/CT data, we transformed attenuation maps to match gated PET data. Simulation studies demonstrate upto 20% improvement in some phases and small to no quantitative improvements in final summed images. A measured patient study shows a quantitative benefit with the proposed Match Slice method. While some quantitative gains can be made for individual respiratory bins, there appears to be little to no benefit in a final summed images.

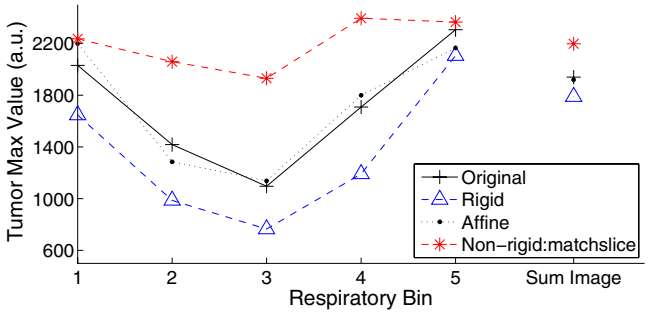

Fig. 10. Maximum value of tumor on apex of right diaphragm in patient study for each respiratory bin and for summed images. Non-rigid method results in constant tumor values across bins suggesting improved quantitative accuracy. Rigid method results in reduced quantitative accuracy.

The results reveal that the consistency of noisy AC-PET data can drive the alignment of the attenuation map and suggests this approach could be applied to all PET to CT alignment errors. The current approaches attempt to transform the attenuation map of the entire chest cavity to each respiratory phase. The apex of the lung is fairly stationary and may be limiting the gains of our methods near the diaphragm. Future work will explore more sophisticated non-rigid transformation methods and limit the transformation volume to a smaller region centered on the diaphragm.

REFERENCES

[1] A. Alessio, J. Caldwell, G. Chen, K. Branch, and P. Kinahan. Attenuation-emission alignment in cardiac PET/CT with consistency conditions. In *IEEE Nucl Sci Symp Conf Record*, volume 6, pages 3288–3291, 2006.

[2] F. Natterer. *The Mathematics of Computerized Tomography*. Wiley, New York, 1986.

[3] N Paquet, A Albert, J Foidart, and R Hustinx. Within-patient variability of 18F-FDG: Standardized uptake values in normal tissues. *J Nucl Med*, 45(5):784–788, 2004.

[4] H Schoder, YE Erdi, K Chao, M Gonen, S M Larson, and H Yeung. Clinical implications of different image reconstruction parameters for interpretation of whole-body PET studies in cancer patients. *J Nucl Med*, 45(4):559–566, 2004.

[5] W.P. Segars and B.M.W. Tsui. Study of the efficacy of respiratory gating in myocardial SPECT using the new 4-D NCAT phantom. *IEEE Trans Nucl Sci*, 49(3):675–679, 2002.

[6] A. Welch, C. Campbell, R. Clackdoyle, and et al. Attenuation correction in PET using consistency information. *IEEE Trans Nucl Sci*, 45(6):3134–3141, 1998.